



Supplement of

Characterization of soot produced by the mini inverted soot generator with an atmospheric simulation chamber

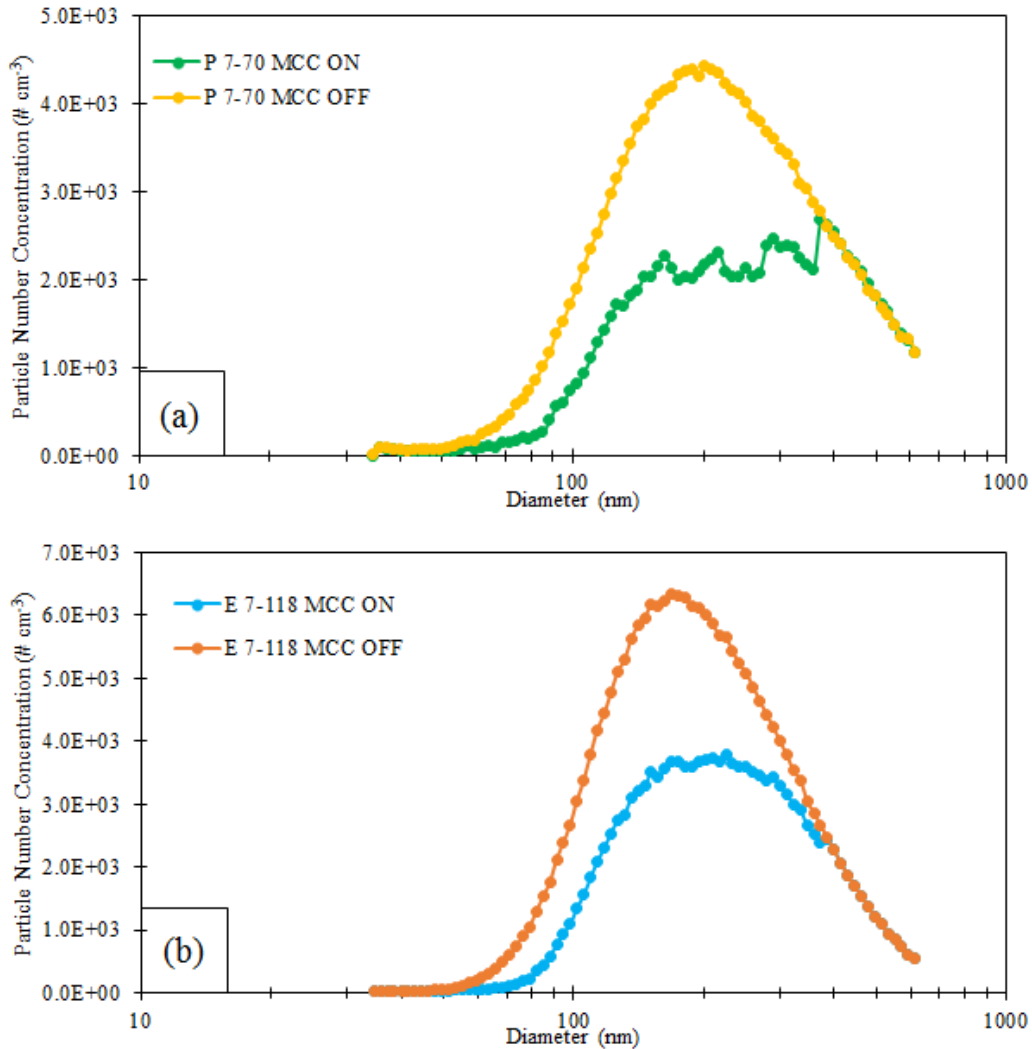
Virginia Vernocchi et al.

Correspondence to: Dario Massabò (massabo@ge.infn.it)

The copyright of individual parts of the supplement might differ from the article licence.

1 **S1. Size distribution measurements**

2 Differences between size distribution corrected and uncorrected by the multiple charge correction algorithm
3 are shown in Fig. S1.



4

5 *Figure S1: Comparison between size distribution corrected (MCC ON) and uncorrected (MCC OFF) by the multiple*
6 *charge correction algorithm of TSI AIM software. Panel (a) refers to propane experiment with 7 lpm of air and 70 mplm*
7 *of fuel. Panel (b) refers to ethylene experiment with 7 lpm of air and 118 mplm of fuel.*

8 **S2. Characterization tests**

9 The categories of flame shape observed in the range of air and fuel flows discussed in sect. 2.1 are summarized
10 in Tables S1 and S2, for propane and ethylene respectively.

11 Table S1: Flame shapes observed for different combustion conditions of propane. Flames are identified as A - asymmetric,
 12 CB - Curled Base, CT - Closed tip, POT - Partially Open tip and OT - Open tip; FL indicates if flickering. The dash
 13 indicates that the flame does not ignite.

		FUEL flow [mlpm]												
		30	35	40	45	50	55	60	65	70	75	80	85	
AIR flow [lpm]	2	A	A/FL	A	A/FL	A	CB/FL	CB/FL	CB/FL	CB/FL	CB/FL	CB/FL	CB/FL	CB/FL
	2.5	A/FL	A/FL	A	A/FL	A/FL	CB/FL	CB/FL	CB/FL	CB/FL	CB	CB	CB/FL	CB/FL
	3	A/FL	A/FL	A	A/FL	A/FL	CB/FL	CB/FL	CB/FL	CB/FL	CB/FL	CB	CB/FL	CB/FL
	3.5	A/FL	A	A	A	A	CB	CB	CB	CB	CB	CB	CB	CB/FL
	4	A	A	A	A	A	CB	CB	CB/FL	CB	CB	CB	CB	OT
	4.5	A	A	A	A	A	CB	CB	CB	CB	CB	CB	CB	OT
	5	A	A	A	A	A	A/CB	CT	POT	OT	OT	OT	OT	OT
	5.5	A	A	A	A	A	CT	CT	POT	OT	OT	OT	OT	OT
	6	A	A	A	A	CT	CT	CT	CT	POT/OT	OT	OT	OT	OT
	6.5	A	A	A	A	CT	CT	CT	CT	POT	OT	OT	OT	OT
	7	A	A	A	A	A	CT	CT	CT	POT	POT/OT	OT	OT	OT
	7.5	A	A	A	A	A	CT	CT	CT	POT	POT/OT	OT	OT	OT
	8	-	-	A	A	A	CT	CT	CT	POT	POT/OT	OT	OT	OT
	8.5	-	-	A	A	A	CT	CT	CT	POT/OT	POT/OT	OT	OT	OT
	9	-	-	A	A	A	CT	CT	CT	CT	POT	OT	OT	OT
9.5	-	-	-	A	A	CT	CT	CT	CT	POT	OT	OT	OT	
10	-	-	-	A	A	CT	CT	CT	CT	POT	OT	OT	OT	

14

15 Table S2: Flame shapes observed for different combustion conditions of ethylene. Flames are identified as A - asymmetric,
 16 CB - Curled Base, CT - Closed tip, POT - Partially Open tip and OT - Open tip; FL indicates if flickering.

		FUEL flow [mlpm]														
		30	35	40	45	50	55	60	65	70	75	80	85	90	95	100
AIR flow [lpm]	2	A	A	A	A	A/FL	A	A	A	CB	CB	CB	CB	CB	CB	CB
	2.5	A	A	A	A/FL	A/FL	A/FL	A	A	CB	CB	CB	CB	CB	CB	CB
	3	A	A	A	A	A/FL	A/FL	A	A	A/CB	CB	CB	CB	CB	CB	CB
	3.5	A	A	A	A	A/FL	A/FL	A	A	A/CB	CB	CB	CB	CB	CB	CB
	4	A	A	A	A	A	A	A	A	A	A/CB	CB	CB	CB	CB	CB/OT
	4.5	A	A	A	A	A	A	A	A	CB	CB	CB	CB	CB/OT	CB/OT	CB/OT
	5	A	A	A	A	A	A	A	A	CB	CB	CB	CB	CB/OT	CB/OT	CB/OT
	5.5	A	A	A	A	A	A	A	A	CB	CB/OT	CB/OT	CB/OT	CB/OT	CB/OT	CB/OT
	6	A	A	A	A	A	A	CT	CT	CT	CT/POT	CT/POT	POT	POT	OT	OT
	6.5	A	A	A	CT	CT	CT	CT	CT	CT/POT	POT	POT/OT	POT/OT	OT	OT	OT
	7	A	A	A	CT	CT	CT	CT	CT/POT	POT	POT/OT	OT	OT	OT	OT	OT
	7.5	A	A	A	A	CT	CT	CT	CT	POT	POT/OT	OT	OT	OT	OT	OT
	8	A	A	A	CT	CT	CT	CT	CT/POT	POT	POT/OT	OT	OT	OT	OT	OT
	8.5	A	A	A	CT	CT	CT	CT	CT	CT/POT	POT	OT	OT	OT	OT	OT
	9	A	A	CT	CT	CT	CT	CT	CT	POT	OT	OT	OT	OT	OT	OT
9.5	A	A	CT	CT	CT	CT	CT	CT	CT	POT	OT	OT	OT	OT	OT	
10	A	CT	CT	CT	CT	CT	CT	CT/POT	POT	POT/OT	OT	OT	OT	OT	OT	

17

18 S3. Comparison between propane and ethylene exhausts

19 We replicated some of the conditions investigated in the previous works (Kazemimanesh et al., 2019; Moallemi
 20 et al., 2019). We explored 9 lpm of air - 100 mlpm of fuel and 10 lpm of air - 100 mlpm of fuel for ethylene
 21 and 8 lpm of air - 61 mlpm of fuel and 9 lpm of air - 61 mlpm of fuel for propane. Results are reported in Table

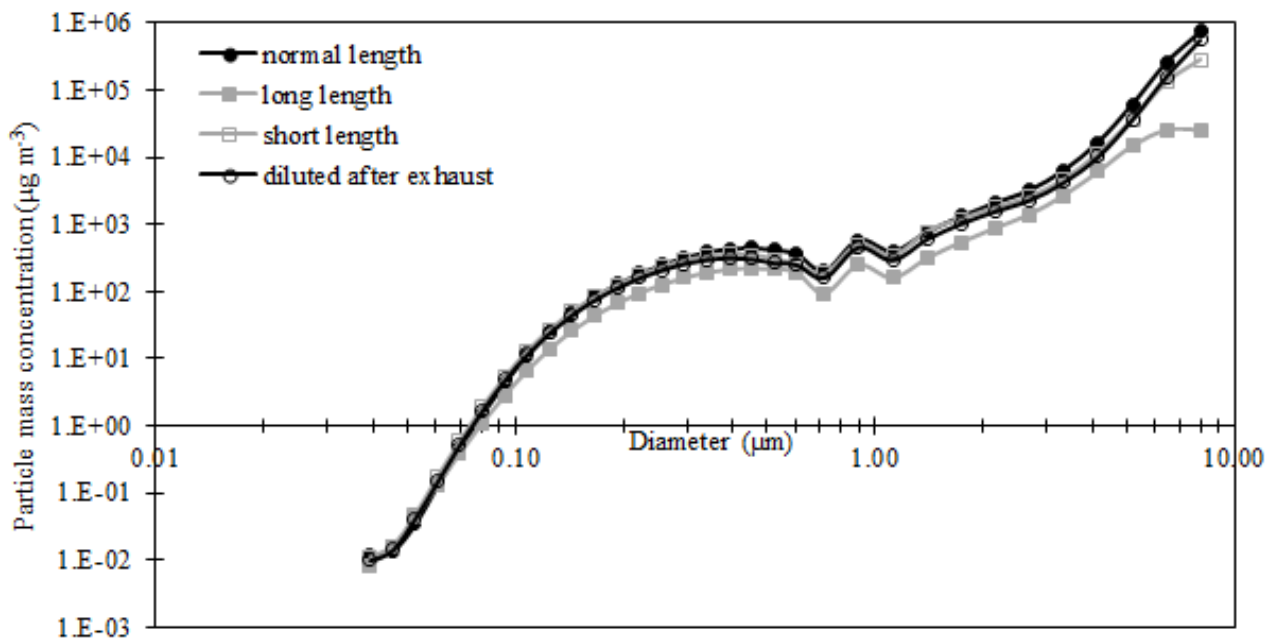
22 S3. Mode diameters retrieved for ethylene experiments, are very close to the values retrieved in
 23 (Kazemimanesh et al., 2019), even if smaller; mode diameters for propane experiments perfectly agreed with
 24 Moallemi et al., (2019) data. Values of SSA-IR resulted similar to the ones in (Moallemi et al., 2019) but a bit
 25 lower. It is important to underline that the setups were different, since our experiments make use of the
 26 simulation chamber, while Kazemimanesh et al., (2019) and Moallemi et al., (2019) measured directly at the
 27 MISG outlet.

28 *Table S3: Comparison between results of previous literature work and our replicated experiments.*

	Kazemimanesh et al., 2019		This work	
	Mode diameter (nm)		Mode diameter (nm)	
Ethylene: 9 - 100	242		191 ± 8	
Ethylene: 10-100	250		220 ± 9	
	Moallemi et al., 2019		This work	
	Mode diameter (nm)	SSA-IR	Mode diameter (nm)	SSA-IR
Propane: 8 - 61	150 - 190	0.17 – 0.22	202 ± 12	0.16
Propane: 9 -61	130 - 160	0.16 – 0.20	165 ± 10	0.14

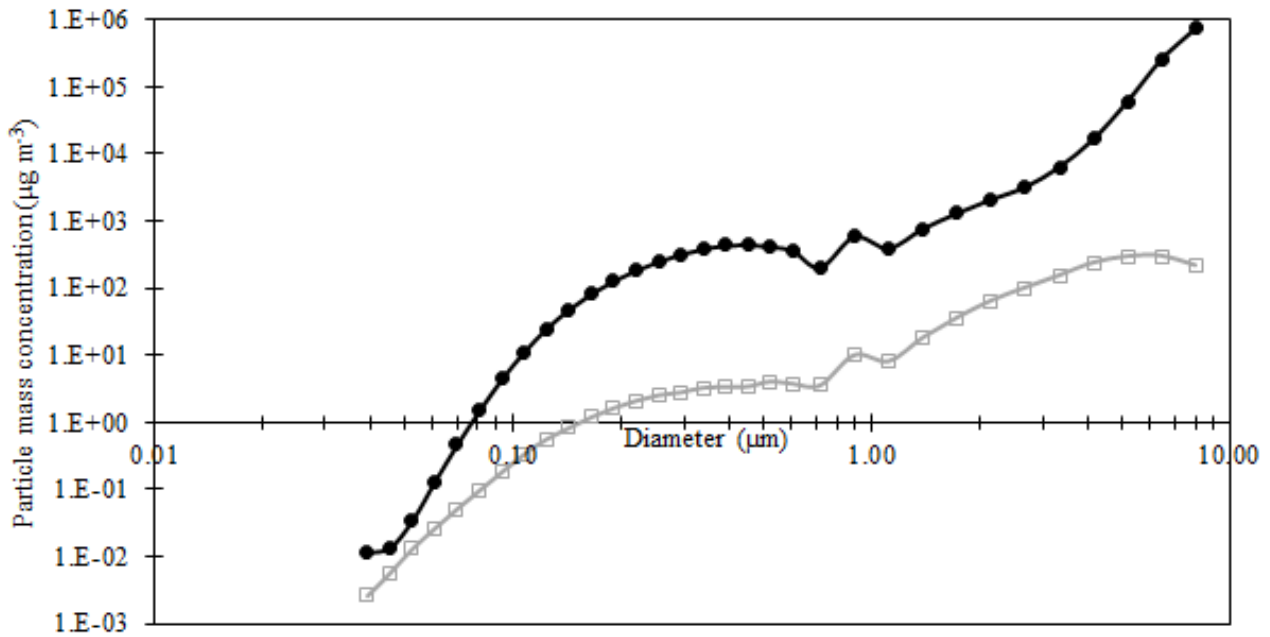
29 **S3.1 Size distribution**

30 To verify the hypothesis that super-aggregates formed at the stagnation plane, some experiments were
 31 performed. The soot generator was fuelled with 7 lpm of air and 127 mlpm of ethylene. Three different line
 32 lengths were used to connect the MISG to ChAMBRe: “normal” (i.e., the same used in Fig. 6) was 65 cm,
 33 “long” was about 5 meters and “short” was 30 cm”. In addition, with the “normal” line, MISG exhaust was
 34 diluted just after the outlet of the generator, by adding an extra air flow; the ratio between dilution air and
 35 MISG generator was 4:1. Only the experiment with the longest line showed a significant decrease in particle
 36 concentration, probably due to the losses inside the pipe (see Fig. S2).



37
 38 *Figure S2: Comparison between mass size distributions measured by SMPS and OPS. The MISG was fuelled with 7 lpm of air and*
 39 *127 mlpm of ethylene.*

40 Super-aggregates formation by ethylene combustion can be partly reduced by using lower air and fuel flow
41 rates, in Fig. S3 a comparison between different flow rates is shown.



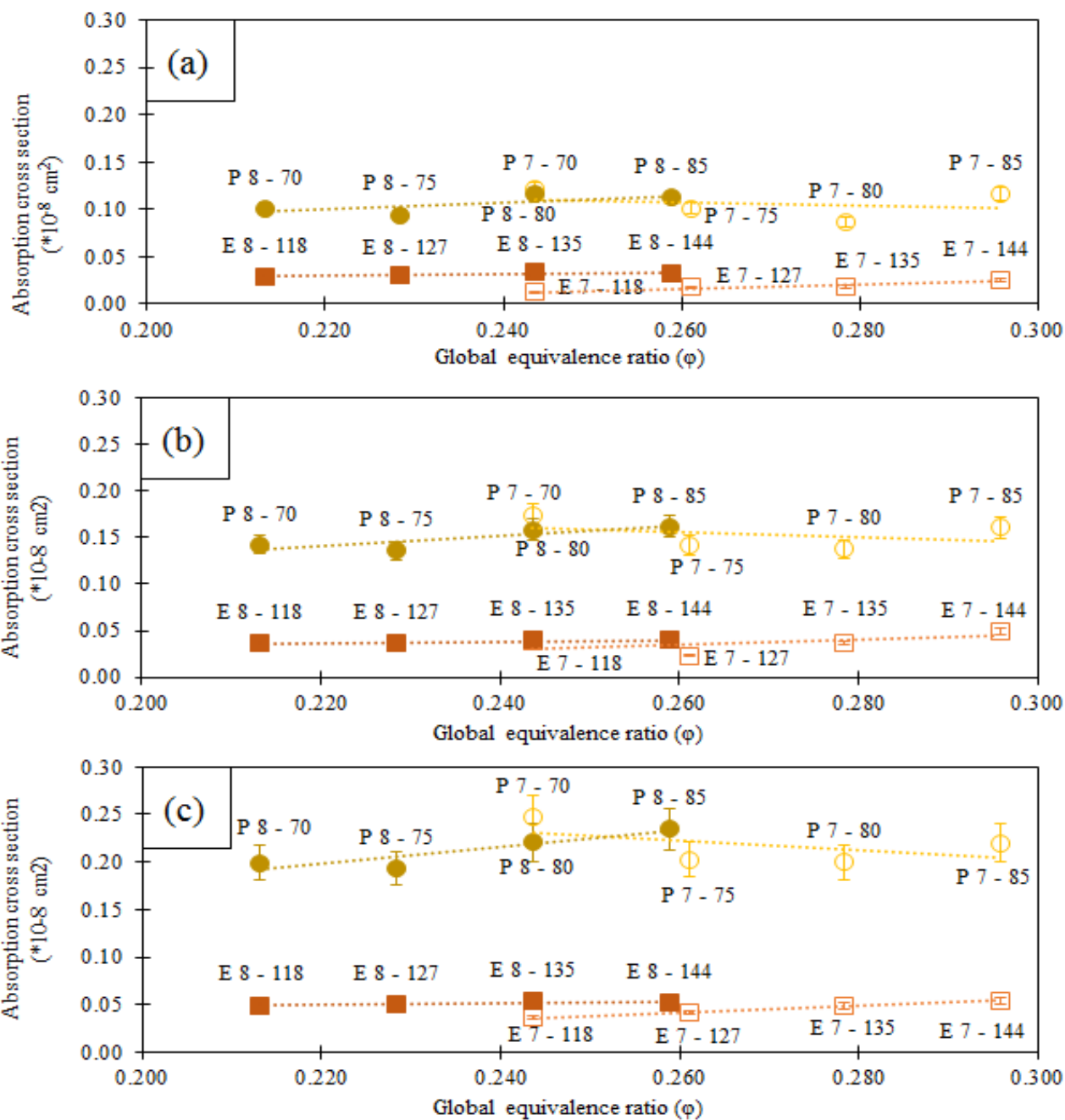
42

43 *Figure S3: Comparison between mass size distributions measured by SMPS and OPS. Black points refer to MISG fed with 7 lpm of*
44 *air and 127 mlpm of ethylene, grey squares refer to MISG fed with 6 lpm of air and 80 mlpm of ethylene.*

45

S3.2 Optical properties

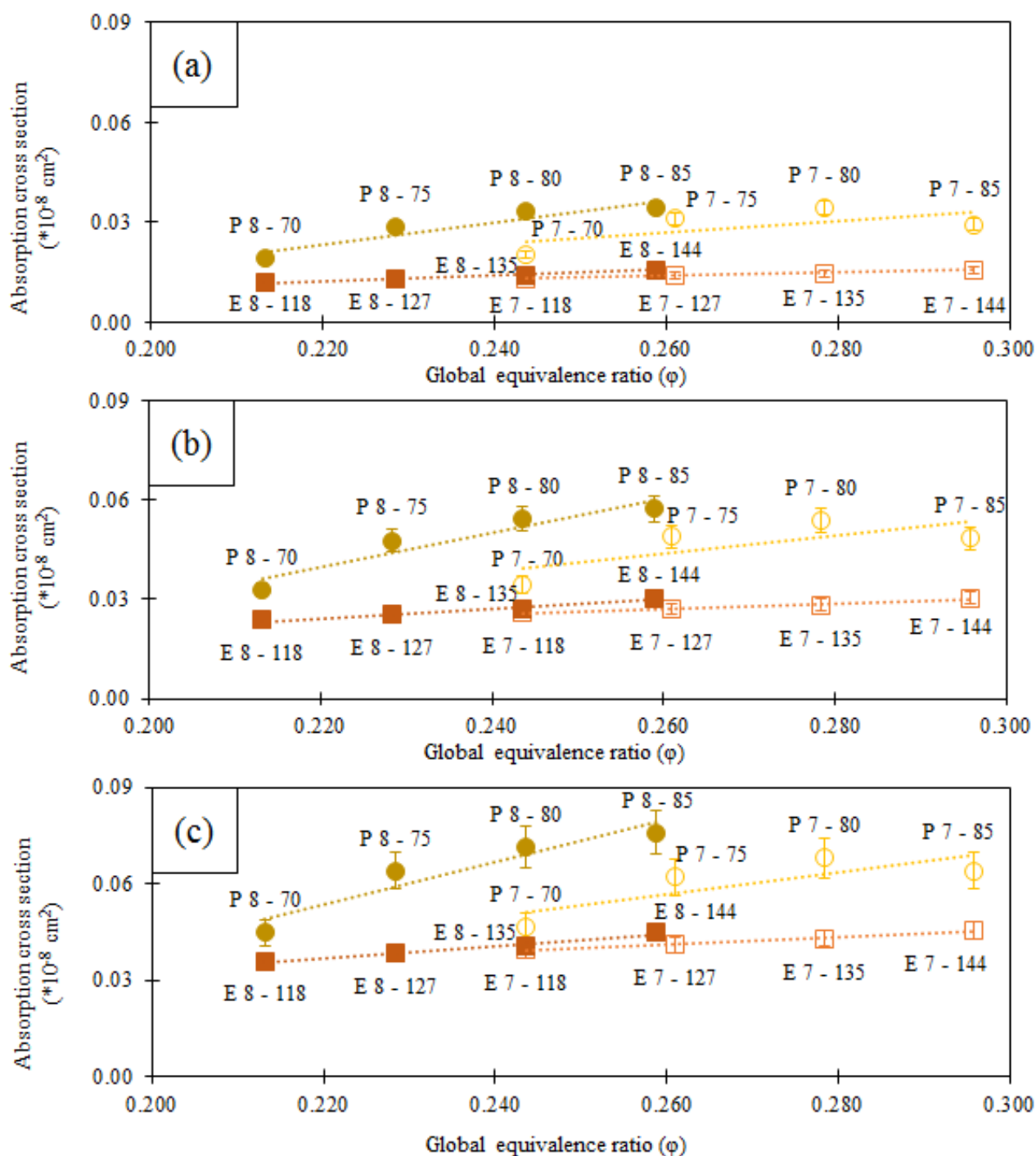
46 The online measured b_{abs} values were normalized to the total particle concentration inside ChAMBRé
47 reached in each single experiment. Absorption coefficients measured at three wavelengths by the PAXs
48 without and with the cyclone mounted upstream, are shown in Fig. S4 and S5, respectively. Each b_{abs} value
49 resulted from the average of 1-second data recorded for a specific time interval (i.e., 4 to 10 minutes).



50

51 Figure S4: Absorption coefficient @ $\lambda = 870$ (a), 532 (b) and 405 (c) nm, measured by PAXs, versus the global
 52 equivalence ratio. b_{abs} values are normalized to the total particle number concentration measured by SMPS in the
 53 corresponding experiments. Experiments were performed without using the cyclone. Each point is labelled by E or P
 54 (ethylene or propane) and a pair of numbers indicating air and fuel flow, respectively in lpm and mlpm. Dotted lines aim
 55 to facilitate the reader eye.

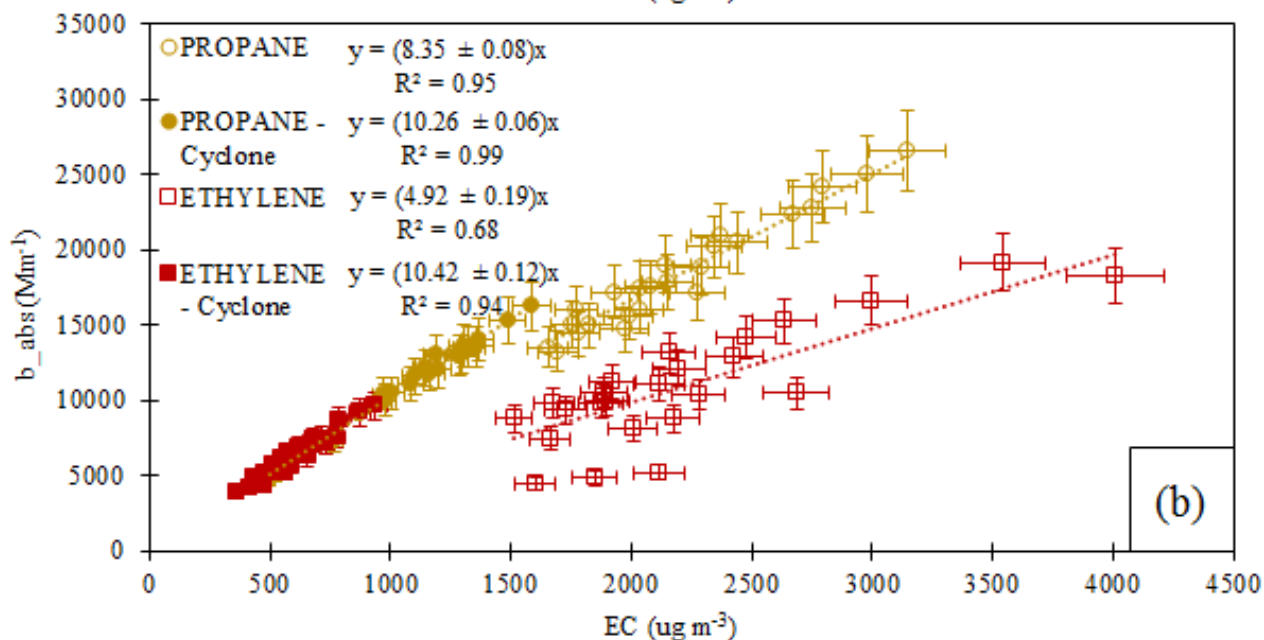
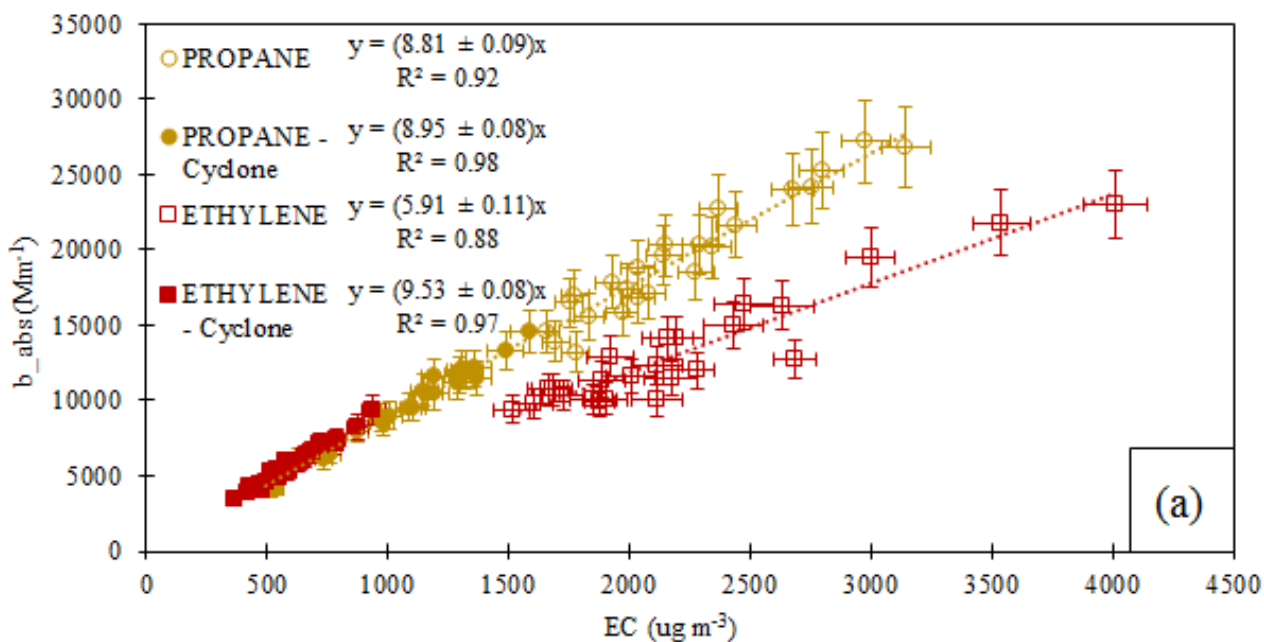
56



57

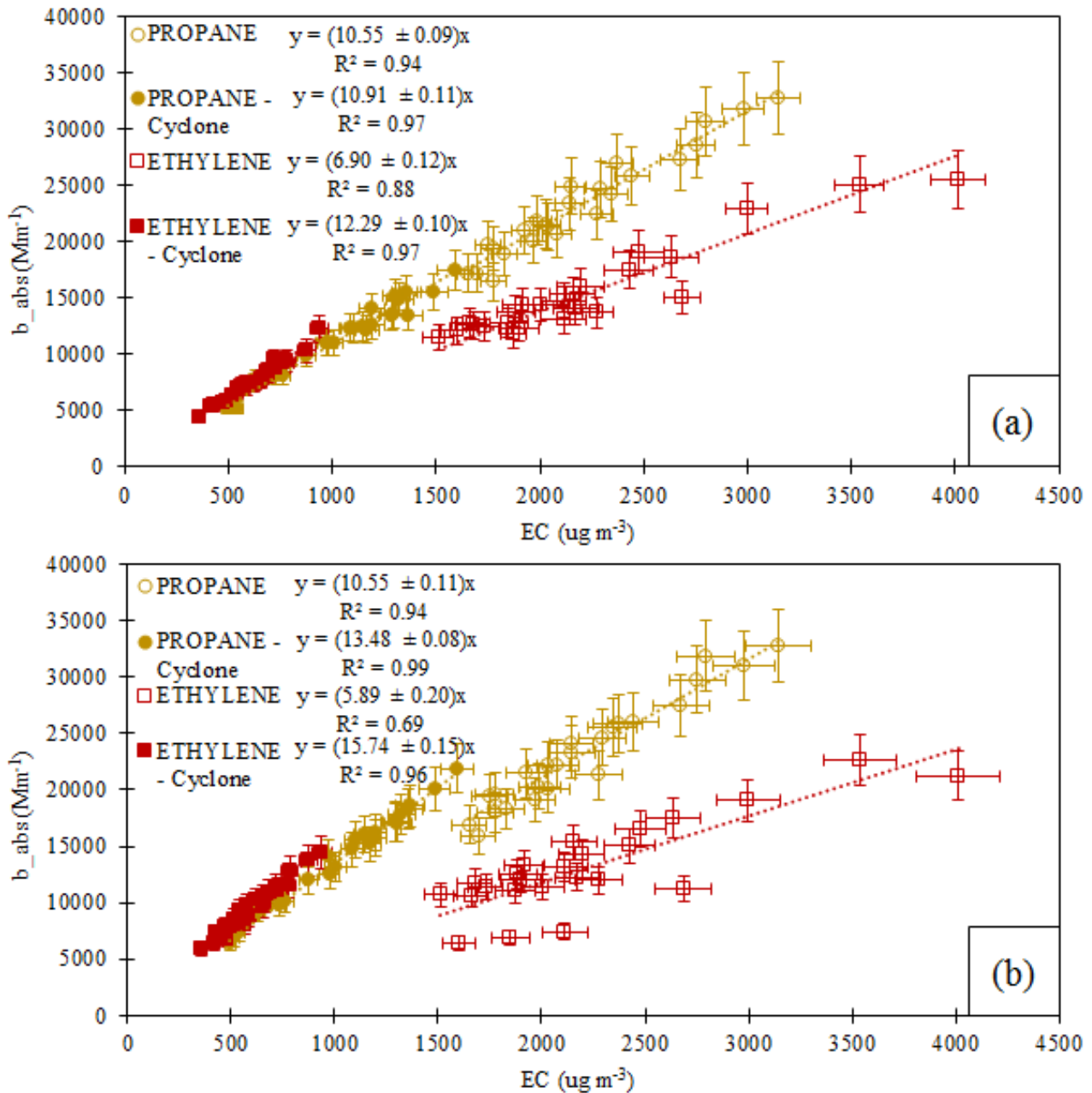
58 *Figure S5: Absorption coefficient @ $\lambda = 870$ (a), 532 (b) and 405 (c) nm, measured by PAXs, versus the global*
 59 *equivalence ratio. b_{abs} values are normalized to the total particle number concentration measured by SMPS in the*
 60 *corresponding experiments. Experiments were performed with the cyclone. Each point is labelled by E or P (ethylene or*
 61 *propane) and a pair of numbers indicating air and fuel flow, respectively in lpm and mlpm. Dotted lines aim to facilitate*
 62 *the reader eye.*

63 The comparison between MWAA and PAXs, at $\lambda = 532$ and 405 nm , on the same carbonaceous aerosol, is
 64 reported in Fig. S6 and S7, respectively. We divided the results by fuel, air flow and with/without cyclone.
 65 Each point in the plots sums-up the observations at different global equivalence ratio values.



66

67 Figure S6: Absorption coefficient @ 532 nm, measured by MWA (a) and PAX (b) versus EC concentration. The slope of
 68 each fit corresponds to the Mass Absorption Coefficient.



69

70 Figure S7: Absorption coefficient at $\lambda = 405$ nm, measured by MWA (a) and PAX (b) versus EC concentration. The
 71 slope of each fit corresponds to the Mass Absorption Coefficient.

72 In Table S4 are reported the 2-wavelength calculations of the AAE for the three PAX units, with the
 73 equation:

74

$$AAE = - \frac{\ln \frac{b_{abs1}}{b_{abs2}}}{\ln \frac{\lambda_1}{\lambda_2}} \quad \text{Eq. S1}$$

75

Table S4: AAE obtained by 2-wavelength calculations from PAX data.

EXPERIMENTAL CONDITIONS	870/532	532/405	870/405
PROPANE 70 to 85 mlpm - AIR 7 lpm	0.91 ± 0.05	0.82 ± 0.09	0.87 ± 0.06
PROPANE 70 to 85 mlpm - AIR 8 lpm	0.94 ± 0.05	0.89 ± 0.09	0.92 ± 0.06
PROPANE 70 to 85 mlpm - AIR 7 lpm - cyclone	0.99 ± 0.07	0.97 ± 0.13	0.98 ± 0.09
PROPANE 70 to 85 mlpm - AIR 8 lpm - cyclone	1.04 ± 0.04	1.07 ± 0.06	1.05 ± 0.05

ETHYLENE 118 to 144 mlpm - AIR 7 lpm	0.95 ± 0.22	0.87 ± 0.42	0.92 ± 0.29
ETHYLENE 118 to 144 mlpm - AIR 8 lpm	0.81 ± 0.03	0.63 ± 0.07	0.75 ± 0.04
ETHYLENE 118 to 144 mlpm - AIR 7 lpm - cyclone	1.35 ± 0.04	1.53 ± 0.06	1.41 ± 0.05
ETHYLENE 118 to 144 mlpm - AIR 8 lpm - cyclone	1.33 ± 0.03	1.51 ± 0.04	1.39 ± 0.04